

EFDA–JET–CP(02)05/05

P. Testoni, F. Durodie, V. Riccardo, P. Sonato, R. Walton
and JET EFDA Contributors

Electromechanical Analyses of the JET ICRH ITER-Like Antenna

Electromechanical Analyses of the JET ICRH ITER-Like Antenna

P. Testoni, F. Durodie, V. Riccardo, P. Sonato, R. Walton
and JET EFDA Contributors*

¹*DIEE-University of Cagliari Piazza d'Armi, I-09123 Cagliari – ITALY*

²*EURATOM-LPP/Ecole Royle Militaire, 30, avenue de la Renaissance, 1000 BRUSSELS, Belgium*

³*EURATOM-UKAEA Fusion Association, Culham Science Centre, Abingdon, Oxfor OX14 3DB, UK*

⁴*Consorzio RFX, Associazione Euratom-ENEA sulla Fusione Corso Stati Uniti, 4, I-35127 Padova (ITALY)*

* *See annex of J. Pamela et al, 'Overview of Recent JET Results and Future Perspectives',
Fusion Energy 2000 (Proc. 18th Int. Conf. Sorrento, 2000), IAEA, Vienna (2001).*

“This document is intended for publication in the open literature. It is made available on the understanding that it may not be further circulated and extracts or references may not be published prior to publication of the original when applicable, or without the consent of the Publications Officer, EFDA, Culham Science Centre, Abingdon, Oxon, OX14 3DB, UK.”

“Enquiries about Copyright and reproduction should be addressed to the Publications Officer, EFDA, Culham Science Centre, Abingdon, Oxon, OX14 3DB, UK.”

ABSTRACT.

A high power and high power density Ion Cyclotron Resonance Frequency (ICRF) antenna is being designed for the Joint European Torus (JET).

3D finite element models of the antenna and neighbouring components (poloidal limiters, the main horizontal port and vessel double wall) have been developed.

The flow pattern of halo currents and the distribution of induced currents during disruptions have been determined with electromagnetic static and transient analyses, imposing loads (rate and amplitude of the poloidal and radial field change and halo current sources) consistent with those observed in the operation of JET. These currents have subsequently been used to estimate the electromechanical loads due to the interaction with the externally imposed magnetic field. Stress, displacements, forces and torques have been calculated in all parts of the antenna subassembly.

1. INTRODUCTION

In a tokamak initial heating of the plasma is provided by the plasma current itself, via ohmic heating. This heating source is reduced as the plasma gets hotter, as its resistivity decreases. Therefore if reactor relevant temperatures are to be reached additional means of heating are required. One of these is the Ion Cyclotron Resonance Frequency (ICRF) system, which couples high power electromagnetic waves to the ions in the plasma.

The paper presents the results of the electromagnetic and structural analyses of the ITER-like ICRF antenna design, due for installation in JET during the 2004 shutdown. This antenna is intended to launch 8MW of RF power at a power density of around 8MW/m^2 [1]. The antenna comprises two poloidal current straps, each subdivided into four electrically short straps complete with in-vessel capacitors. The antenna is supported via a box cantilevered to the external support structure. The antenna is installed using Remote Handling. Plug-in replacement of the capacitors is performed through the vacuum vessel port [2].

The complexity of this structure together with the non-uniformity of the magnetic field makes Finite Element (FE) modelling the most suitable way for assessing its structural integrity. The Magnetic Vector Potential (MVP) formulation has been used to calculate the eddy current pattern in all the conductive materials, while the Electric Scalar Potential formulation has been used for the halo current distribution. These currents, via Lorentz forces, have been used to evaluate the antenna loads, which have been applied as nodal loads.

2. CALCULATION TECHNIQUE AND MODEL

The FE model (Fig.1) includes the antenna and the main in-vessel components near it. Most of the antenna components are made of inconel 600 ($\rho = 103 \cdot 10^{-8} \Omega \text{ m}$). The antenna housing is 2mm thick and corrugated in toroidal direction. The corrugation is simulated with a non-isotropic resistivity. The housing dimensions are 1.3m in poloidal direction, 0.74m in toroidal direction and 0.147 m in radial direction.

The eight straps are 2mm thick along the plasma side and 1 mm elsewhere. Straps have been modelled like solid conductors. The antenna box is 6mm thick. The housing is connected to the antenna box by 12 contacts, which simulate the bolts.

Five toroidal septa are welded to the sidewalls and the back wall of the housing, they are 10mm thick. A septum at the vertical symmetry plane of the housing is 5mm thick. The line of elements at the tip of the vertical septum, where the beryllium bars are fixed, is made of a fictitious material to account for staggering. The 24 Beryllium ($\rho = 8 \cdot 10^{-8} \Omega\text{m}$) bars of the screen have a section of $24 \times 24 \text{ mm}^2$. In the model the poloidal limiters have been considered with the real height and weight, but the section has been homogenised. The two poloidal limiters have been linked (above and below the antenna) by inconel 625 ($\rho = 130 \cdot 10^{-8} \Omega\text{m}$) tubes. The tube outer radius is 40 mm and the inner radius is 30 mm. Two low resistance contacts connect the link to the housing surface ($30 \mu \Omega$) and the vessel ($20 \mu \Omega$). Thirteen electrical resistors of $3\text{m}\Omega$ each connect the antenna housing to each poloidal limiter. Six electrical resistors of $3\text{m}\Omega$ connect the poloidal limiter with the vessel wall. The two vessel walls are made of inconel 600, 16mm thick and spaced 28mm. The vessel bellows are made of inconel 625. Each bellow is 2mm thick and 0.352m long (real toroidal length), in the model an equivalent non-isotropic resistivity has been used. The main port is 12mm thick and made of inconel 600. Where the component model dimensions are different from the real ones an equivalent resistivity has been used.

The mathematical formulation chosen to calculate the halo current distribution, the Laplace's equation $\nabla^2 V = 0$, requires one degree of freedom per node (the voltage).

The eddy current distribution has been calculated by the magnetic vector potential formulation which involves the solution of the following differential equations:

$$\nabla \times [\nu] \nabla \times \vec{A} = J_s$$

in all non-conductive domains, and

$$\nabla \times [\nu] \nabla \times A + [\sigma] \cdot \left\{ \frac{\eta \vec{A}}{\eta t} + \nabla V \right\} = J_s$$

in the conductive domains. Three degrees of freedom per node (the magnetic vector potential components) are present in non-conductive domains while in conductive domains an additional degree of freedom (the electric scalar potential) is needed. Symmetry allowed to implement a finite element model which only takes into account a quarter of the antenna for the induced current calculation. This formulation requires modelling of a large volume around all the conductive materials.

Subsequently, structural analyses have been performed to determine displacements, stresses and reaction forces, under static loading conditions, with a FE model consisting only of the antenna components.

3. APPLIED LOADS AND BOUNDARY CONDITIONS

In the eddy current calculations, two load cases have been taken into account: poloidal (120T/s)

and radial (80T/s) field variation [3]. The forcing field has been applied through the boundary conditions on the vector potential. This is sufficient to give the correct eddy current pattern inside the conductive materials. The force loads are evaluated in a second step using properly off-set values of the magnetic field.

Figure 2 shows the magnetic field distribution during a poloidal field variation (120T/s obtained from a swing of 0.9T in 7.5ms), here the magnetic field shielding due to the eddy current circulation in the vessel walls is clear. After 0.0075s the magnetic field inside the torus is between 0.9 and 1T, while outside is less than 0.2T.

The halo current distribution has been calculated in a steady-state analysis by applying an electric current as a nodal load. The following current values have been applied:

- 42 kA in the upper quarter of the screen bars
- 12 kA on the upper quarter of the right poloidal limiter on the half plasma facing surface closest to the antenna
- 12 kA on the upper quarter of the left poloidal limiter on the half plasma facing surface farthest from the antenna.
- 159 kA on the upper quarter of the left poloidal limiter on the side farthest from the antenna.

Zero voltage has been imposed at the boundaries of the model (the vessel walls).

Figure 3 shows the voltage distribution due to the halo current loads. The maximum is 20.7V and this is in the upper side of the left poloidal limiter, where most part of the current is applied.

The electromechanical loads due to the current distribution crossing the magnetic field (1T poloidal, 0.6T radial, the toroidal field inversely proportional to the radius and 4T at 2.96m) have been applied as nodal loads for the structural analysis. The rear plate of the antenna box has been constrained in all the directions.

4. RESULTS

4.1 EDDY CURRENT DISTRIBUTION

During the vertical field variation most of the eddy current flows toroidally along the vessel wall. Where the antenna is installed, this offers a parallel path for the toroidal current. This current goes from the vessel wall to the antenna and to the poloidal limiter through the resistive contacts. The toroidal current, 53.6kA, splits between the poloidal limiters' links (31.2kA) and the resistive contacts between the antenna housing and the poloidal limiter (22.2kA). The current entering the antenna is uniformly distributed among all the contacts. The current, from these contacts, flows mainly in the bars and only a small fraction goes in the three septa. Also the bar currents are rather uniformly distributed. The sum of the bar currents is 70.2kA, while the net current in all septa is 2.2kA. A part of the current flowing in the front of the antenna goes to the vessel wall, the rest closes the loop in the back wall of the antenna housing (2kA) and in the box walls through the contacts between the housing and the box (50.2kA).

During a radial field variation the current flows in loops normal to the radial direction, mainly in

the large one made of the poloidal limiters and their links. The current flowing vertically along the poloidal limiter is about 43kA. Most of it closes its loop through the poloidal limiters' link, the rest goes to the contacts between the housing and the poloidal limiter: the maximum value is at the top contact (1.05kA), the minimum, close to zero, in the mid-plane contact. The current transferred from the poloidal limiter to the vessel wall is negligible. Another current loop is made of the beryllium bars and the sides of the antenna housing. In the bars the current increases from close to zero at the mid plane to the top (6.13kA). The current at the vertical symmetric plane of the antenna is 28.2kA, of which 14.2kA flow in the antenna housing. The current in the antenna box, which flows around the radial direction, is 92.2kA.

4.2 HALO CURRENT DISTRIBUTION

A part (33kA) of the total current (171kA) applied on the left poloidal limiter goes in the antenna through the contacts between the housing and the poloidal limiter. Another part (23kA) of this current arrives in the vessel wall through the contacts between the vessel and the poloidal limiter, the remaining part (115kA) goes to the poloidal limiter's links.

The current applied to the antenna bars (42kA) and the one coming from the left poloidal limiter goes in the vessel wall through the low resistance contacts at the poloidal limiter's links (30kA), to the right poloidal limiter (5.2kA) and in the box walls through the bolts (39.2kA). The current flows from the box bolts to the box walls (26.4kA) and to the central cross of the box (12.8 kA) and comes back through the main port walls (39.3kA). In the left side of the beryllium screen the current goes along the bars from the housing walls to the vertical septum. In the right side the current splits from the centre to the ends where bars are loaded and goes from the central septum to the housing walls elsewhere. The highest bar currents are on the right side where the input current is higher and in the bottom left side where current flows from the poloidal limiter. The maximum current value in bars is 1.8kA, the minimum is close to zero.

The current applied on the right poloidal limiter (12kA) and that one which comes from the housing (5.2kA) goes to the vessel through the poloidal limiter-vessel contacts (6.7kA) and to the poloidal limiter's link (10.5kA). The current flowing in the low resistances between the poloidal limiter's links and the vessel wall is 150 kA.

4.3 STRESSES, DISPLACEMENTS AND REACTIONS

Results of the structural analysis show that stresses in all part of the structure are under the materials yield strength limit except around connection points between the housing and the box of the antenna. The forces, due to the eddy currents and Halo currents loads, in radial, poloidal and toroidal direction applied at the support at the back of the box are showed in Table 1:

The analysis provided the following results:

- The screen bars deformation has a maximum value of 1.7mm, the maximum Von Mises stress is 10 MPa.

- Stresses in the housing and in the box are high in the regions where they are connected together elsewhere stresses are well under the yield strength limit.
- The maximum deformation in the housing is 3.5mm and in the box is 1.3mm; both are in the bottom.

	Fr [kN]	Fp[kN]	Ft[kN]
Eddy current load	17	10	0
Halo current load	38	90	67

Table.1 Reaction forces

CONCLUSIONS

The results of the analyses validated the selection of resistances between the antenna housing and the in-vessel components, aiming to avoid high current densities in all the antenna components. The mechanical analyses showed that stresses in all parts of the structure are under the materials yield strength. The computed reactions served as an input to design the mechanical structure supporting the antenna and its components.

ACKNOWLEDGEMENTS

This work was supported in part by Euratom and was performed under the European Fusion Development Agreement.

REFERENCES

- [1]. F Durodie et al., JET-EP ITER-like ICRF antenna., 14th Topical Conference on Radio Frequency Power in Plasmas, Oxnard, 7-9 May 200.
- [2]. R Walton et al., Mechanical design of the ICRH antenna for JET-EP 19th IEEE/NPSS Symposium on Fusion Engineering, Atlantic City, 22-25 January 2002.
- [3]. V Riccardo et al., Disruption design criteria for the JET in-vessel components 19th IEEE/NPSS Symposium on Fusion Engineering, Atlantic City, 22-25 January 2002.

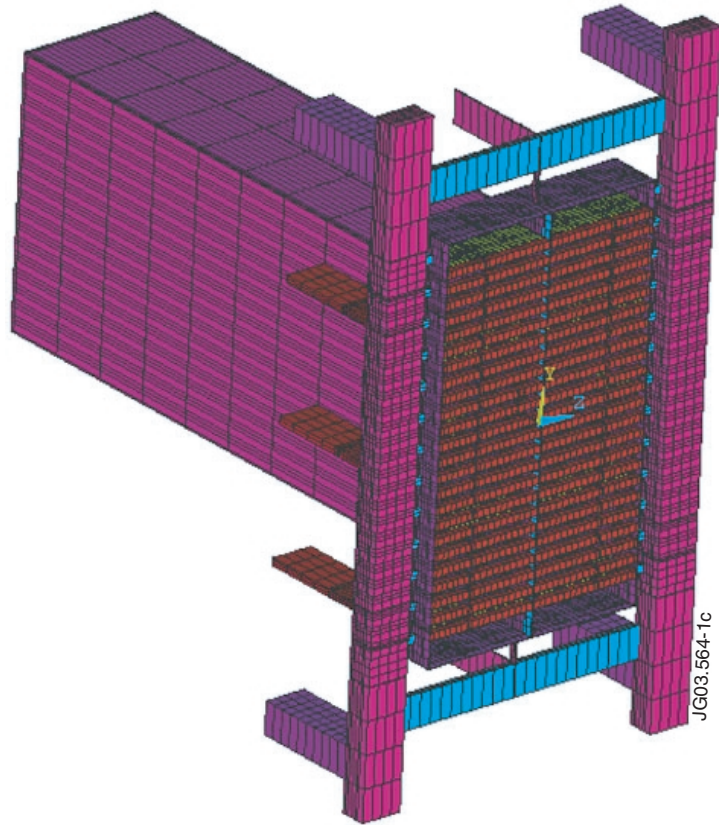


Figure 1: Model of the ITER-like ICRF antenna.

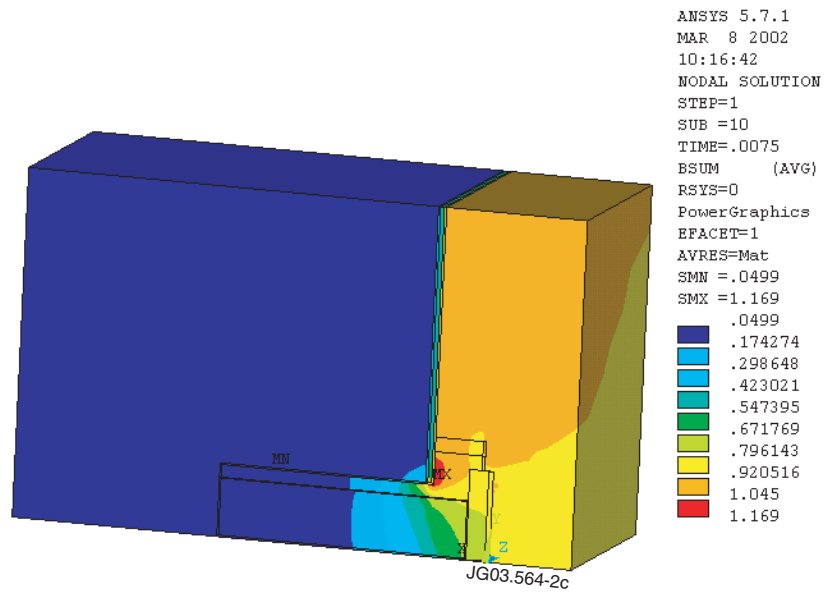


Figure 2: Poloidal magnetic field variation.

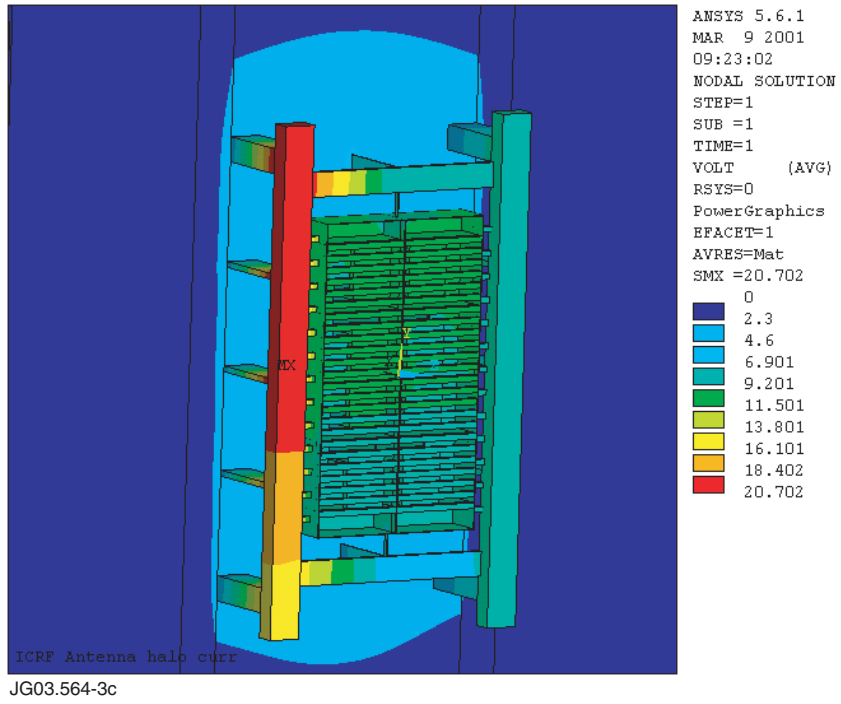


Figure 3: Potential distribution due to the halo current.